

Quantum dots as single-photon sources: Antibunching via two-photon excitation

Matthias D. Wissert, Birgit Rudat, Uli Lemmer, and Hans-Jürgen Eisler*

DFG Heisenberg Group Nanoscale Science, Light Technology Institute (LTI), Karlsruhe Institute of Technology (KIT), DE-76131 Karlsruhe, Germany

(Received 5 January 2011; revised manuscript received 4 February 2011; published 15 March 2011)

Two-photon excitation induced photoluminescence (2PE-PL) microscopy of CdSe colloidal quantum dots at the single-entity level is demonstrated. We provide evidence for single nanoparticle microscopy in the two-photon excitation regime by varying the laser excitation average power, as well as by measuring the confocal point spread function in three dimensions with a single quantum dot. Model calculations of the point spread function are in good agreement with our experimental findings in the 2PE-PL nonsaturation regime. Ultimately, we observe photon antibunching and triggered single-photon emission at room temperature from those quantum nanostructures under two-photon excitation in a well-defined three-dimensional photonic volume.

DOI: [10.1103/PhysRevB.83.113304](https://doi.org/10.1103/PhysRevB.83.113304)

PACS number(s): 73.21.La, 42.50.Ar, 78.67.Bf, 03.67.—a

While two-photon absorption had been theoretically described by Maria Göppert-Mayer as early as in 1931,¹ the field of two-photon excitation microscopy was only opened by W. Denk *et al.* in 1990.² It is of specific interest for many characterization purposes such as subcellular and medical imaging since it can provide a large spectral distance between the excitation light and the observed photoluminescence of suitable chromophores. It thus enables straightforward wavelength filtering, confines the optical detection capability in three dimensions due to its inherent quadratic intensity dependence, and offers improved imaging contrast due to decreased scattering, NIR absorption, and fluorescence in biological environments. Moreover, it can be advantageous in spectroscopy and microscopy for excited-state symmetry selection rule studies.

The two-photon excitation imaging technology triggered the search, creation, and characterization of favorable chromophores³ with low intensity two-photon laser excitation conditions together with long observation time scales. Such organic fluorophores, however, show low two-photon excitation cross sections together with rapid photobleaching properties⁴ compared to the colloidal semiconductor CdSe nanocrystals used here (also referred to as quantum dots), with a two-photon excitation cross section as high as 66 000 GM (Göppert-Mayer units GM = 10⁻⁵⁰ cm⁴ photon/s).⁵ Also, semiconductor quantum nanostructures show at the single-entity level strong photoluminescence rates under ambient conditions that favored quantum optics experiments such as photon antibunching under one-photon excitation⁶⁻⁸ and even triggered single-photon emission under pulsed one-photon absorption.⁹ Fine tuning and an energetic smoothing of the interface of the core-shell nanostructure have recently lead to nonblinking semiconductor nanocrystals with photoluminescence excited-state lifetimes in the range of 4.0–5.6 ns.¹⁰

Although single-photon sources and antibunching mediated by two-photon absorption of a coherent laser beam have been proposed theoretically as early as in 1975,^{11,12} a proof-of-concept experiment is still missing. This is commonly attributed to the lack of appropriate chromophore systems with high 2PE cross section combined with high photostability.¹³ Such experiments are of fundamental interest as they enable deeper insight into sub-Poissonian photon statistics, i.e., so-called strict and temporal antibunching that might be

achievable with appropriate photonic devices.¹⁴ Moreover, on the single quantum light source side, two-photon excitation microscopy would allow us to study the photon statistics of competing photoluminescence and nonradiative relaxation rates of nonergodic chromophores¹⁵ (such as colloidal quantum dots⁸) deeply, extensively, and addressable in a three-dimensional (3D) photonic volume.

Colloidal semiconductor nanocrystals as single chromophores at room temperature should be able to act as single-photon sources under two-photon excitation conditions, an experiment that has not been demonstrated so far. In this work, we take the steps on the experimental side to address the two-photon excitation scheme of a single quantum dot at ambient conditions to demonstrate antibunching and triggered single-photon source capability.

We expect this type of excitation to be relevant to optical quantum computing¹⁶ in 3D and quantum cryptography¹⁷ in 3D, specifically where high numbers of single-photon sources need to be placed in small photonic volumes, since two-photon excitation provides smaller excitation dimensions ($\approx\lambda/3$) for single-photon generation on demand. Moreover, coupling colloidal quantum dots with optical gold nanoantennas¹⁸ shall pave the way for triggered single-photon sources with *directional* photon emission properties using one 2PE beam.

The synergy of optical two-photon excitation, three-dimensional optical detection capability, photoluminescence intensity maps, lifetime images of nanocrystals, and triggered single-photon sources at room temperature is demonstrated in this paper. We not only confirm that such two-photon excited photoluminescence can be produced in colloidal CdSe quantum dots in a well-defined 3D photonic volume, but also show that photon antibunching can be observed for such a single nanocrystal at room temperature with high stability.

For this study, we used CdSe nanocrystals emitting photoluminescence with a peak wavelength around 605 nm and an ensemble relative quantum yield between 40% and 50%. For the single chromophore studies here, the quantum dots were diluted to 10⁻¹⁰ molar and thereafter drop casted onto a clean standard glass cover slip (thickness 170 μ m). The glass sample was covered with an additional polymethyl methacrylate (PMMA) layer (approximately 100 nm thick) on top to immobilize the nanostructures. Thereafter, the sample was two-photon illuminated by an 810 nm (peak-power

wavelength) Ti:sapphire laser. The polarization of the excitation laser light was set to circular by means of a combination of $\lambda/4$ - and $\lambda/2$ -wave plates. To achieve a high-quality focus, the collimated excitation light was expanded for a good overfill (factor $2.5\times$) of the aperture of a $100\times$ (NA 1.46) objective lens (Zeiss). The sample position with respect to the laser focus could be controlled using a three-axes piezocrystal stage (TAO-Stage, JPK Instruments). For the detection channel, the same objective lens was used. We separated the excitation laser light with a dichroic mirror from the photoluminescence (PL). The two-photon induced PL of a single quantum dot was recorded using two single-photon avalanche photodiode (APD) detectors (EG&G) by point-by-point measurements of the sample. The APD detectors were connected to a photon counting card (SPC 830, Becker & Hickl), which enabled digital readout of the single-photon stream. Splitting the PL of a single quantum dot by a 50 : 50 nonpolarizing beam splitter comprises a so-called Hanbury Brown and Twiss detection device.¹⁹ We could thus measure the photon-pair coincidence histogram for our colloidal semiconductor nanocrystals.

To provide experimental evidence for the two-photon process, we confirmed that (i) the photoluminescence intensity or PL rate R obeys a square dependency on the excitation laser intensity I (Fig. 1); (ii) additionally, we took a 3D image of the confocal point spread function, which is a convolution of the excitation point spread function and the detection point spread function (Fig. 2); and (iii) finally, we performed antibunching measurements on a single quantum dot [Fig. 3(c)] from a raster-scanned nanocrystal sample. These raster-scanned images contain as the imaging contrast the number of photons per time bin [pixel information in Fig. 3(a)] as well as the lifetime information from those time bins. Each pixel information in Fig. 3(c) is therefore a result of a single exponential fitting procedure using a maximum likelihood estimate (MLE).

In Fig. 1, the quantum-dot photon photoluminescence intensity is plotted versus the laser excitation power. With an average laser power I from $3\ \mu\text{W}$ to about $50\ \mu\text{W}$ at 810 nm (at 76 MHz laser repetition rate and an approximate

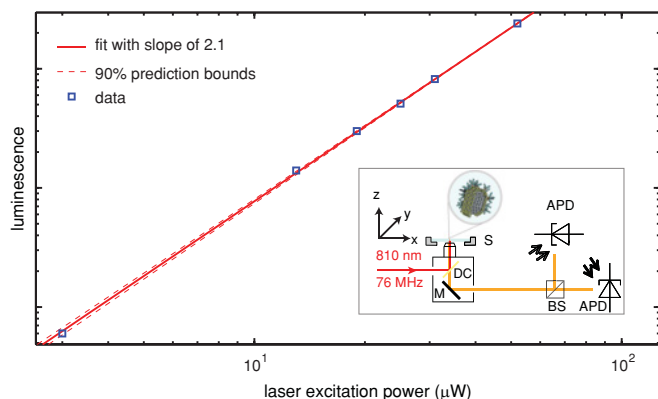


FIG. 1. (Color online) Double logarithmic plot of the laser excitation power vs the PL luminescence rate showing a slope of two. Inset: Schematic of the experimental setup used. The photoluminescence of a single quantum dot sample (S) is sent through a dichroic mirror (DC) and a mirror (M) into a Hanbury Brown and Twiss detection device comprising two avalanche photo diodes (APD) connected by a 50:50 beam splitter (BS).

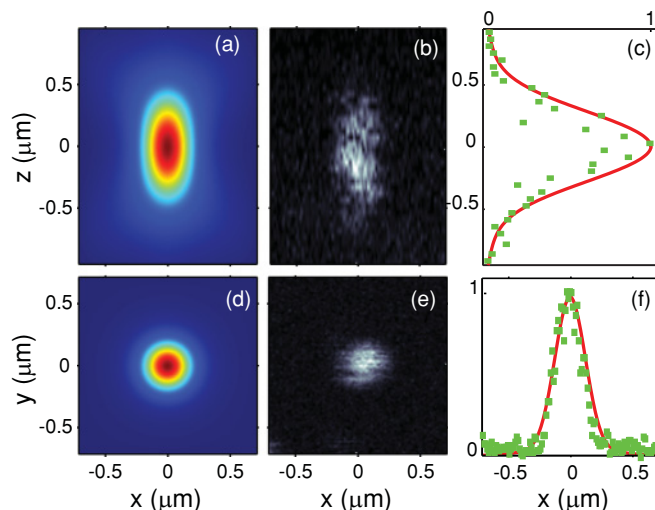


FIG. 2. (Color online) (a) and (d) show the model of the confocal point spread function (PSF); (b) and (e) show the confocal point spread function measured with a single quantum dot as the probe; (c) and (f) show the comparison (normalized) of the model PSF [solid line; line cut through center of (a) and (d)] with the experimental PSF [scattered points; cut through center of (b) and (e)].

pulse width of 500 fs at the laser focus) applied to a single quantum dot, we measured a PL rate R that scales nicely as a square dependence. The rate equation $R = R_\infty \frac{(\frac{I}{I_{\text{sat}}})^2}{1 + (\frac{I}{I_{\text{sat}}})^2}$ is thus applied in a range where the average laser power used is clearly well below the saturation regime $I_{\text{sat}} \stackrel{\text{def}}{=} \frac{1}{2} R_\infty$. We also benefit from the fact that those semiconductor nanocrystals have among the available 2PE chromophore systems the highest 2PE cross section measured so far.⁵ This relaxes the experimental fine adjustment for improving 2PE induced PL generation efficiency by pulse compression devices near the focal region.

It has been shown experimentally that 2PE cross sections on the order of 66 000 GM for CdSe quantum dots at room temperature do easily start to saturate the confocal detection volume, yielding a confocal volume that is largely extended.⁵ Therefore, we applied a laser average power well below saturation I_{sat} to measure the confocal point spread function of our optical microscope with a single quantum dot as a local delta-type probe. The nonsaturation regime of the laser power used here is translated into a measurement of the confocal point spread function, as depicted in Fig. 2. To achieve this, we used the three-axes piezostage available to generate a stack of raster images of the optical PL response of a single quantum dot to the excitation laser focal volume. Images of size $1.5\ \mu\text{m} \times 1.5\ \mu\text{m}$ were taken in 50-nm steps. The three-dimensional resolution capability of 2PE-PL is nicely verified with our home-built confocal microscope. The quantum dots are extremely stable over time, and no degradation is observed throughout the data acquisition time (<1.5 h). We still observe minor blinking effects of our nanocrystals.²⁰ Nevertheless, we find good agreement between our measured point spread function under 2PE conditions and a model with a kernel based on an algorithm for a fast focus field calculation,²¹ which takes into account evanescent field

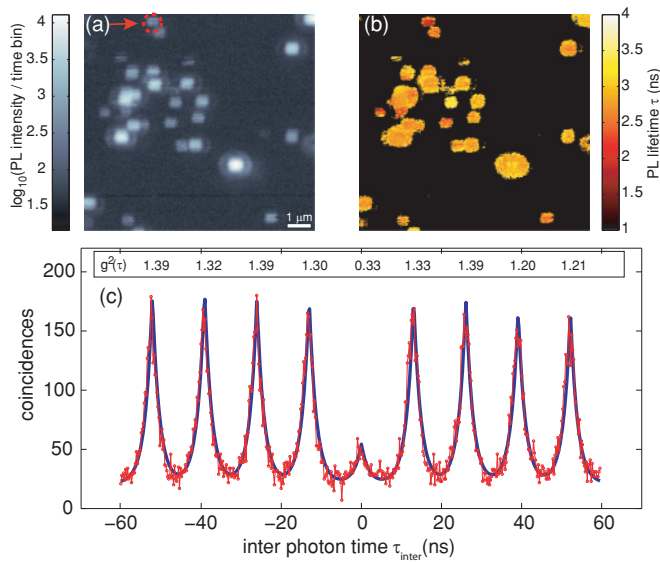


FIG. 3. (Color online) (a) Photoluminescence intensity image of quantum dots via two-photon excitation at room temperature (scale bar 1 μm , typical PL count rate 500 000 photons/s for a single quantum dot at ambient conditions); (b) corresponding photoluminescence lifetime information image; and (c) coincidence measurement of PL photon pairs of a single quantum dot [arrow in (a)] using a Hanbury Brown and Twiss detection device (connected points). The coincidence measurement is fitted with a sum of single exponentials (solid line) yielding an apparent excited-state lifetime for this single quantum dot of $\tau = 1.7$ ns. The normalized coincidence curve yields the intensity autocorrelation function $g^2(\tau_{\text{inter}})$ with numeric values above each peak.

contributions for specifically polarized input fields, as well as all the pertaining optical parameters: high NA, effective refractive index of the quantum-dot embedding medium $n_{\text{eff}} = 1.5$, the polarization state of the incoming laser, the excitation wavelength, the emission wavelength, the Gaussian beam shape, and microscope objective overfill. The model predicts a FWHM in the x, y plane near the focus of ≈ 285 nm and in the x, z plane of ≈ 657 nm. As model and measurement agree nicely here, we can state that the major contribution to the confocal point spread function stems from the intensity square dependency of the excitation point spread function, which is not the case for all nanoscale systems involving square-dependent excitation-luminescence profiles.²²

Finally, we have observed the two-photon excitation induced photoluminescence antibunching behavior of colloidal CdSe quantum dots at room temperature from a raster-scanned sample, as depicted in Fig. 3(a). Such behavior was observed for a single quantum dot ($N = 1$) if placed into the confocal laser excitation volume [Fig. 3(c) and as indicated in Fig. 3(a), arrow]. Clearly, the reduced photon-coincidence peak strength at the interphoton time $\tau_{\text{inter}} = 0$ indicates that we do observe the antibunching effect for a single semiconductor nanocrystal at room temperature under 2PE. The coincidence maxima in Fig. 3(c) derive from the fact that the two-photon induced PL was generated by excitation with a pulsed laser. The distance between peaks therefore yields the repetition frequency of 76 MHz. It is apparent that the

correlation function does not drop all the way down to the zero level in-between the coincidence maxima. We tentatively explain this interphoton signal background by coincidence contribution from the substrate due to nonperfect spectral filtering under the pulsed high peak power in the focal region, the intrinsic detector background noise level, and the finite-time resolution of the experiment (here, 100 ps). Furthermore, we can not exclude photon-pair coincidence contributions from multiexciton radiative relaxations for $\tau_{\text{inter}} = 0$ for this size of CdSe nanocrystals.²³

We obtain the intensity autocorrelation function $g^2(\tau_{\text{inter}})$ by normalizing²⁴ the experimental coincidence curve. The normalization can be obtained by dividing the total number of time intervals measured (acquisition time) by the product of the mean photon counts of our two APD detectors. Therefore, we get a normalized area of the peak values with $g^2(\tau_{\text{inter}}) > 1$ at $\tau_{\text{inter}} \neq 0$ pointing toward the well-known additional bunching effect mediated by the metastable quantum-dot blinking states (on and off states). Consequently, quantum-dot blinking or intermittency shows no characteristic time scale over which a photoluminescence intensity average for nanocrystals can be given; they are nonergodic.⁸

For $g^2(\tau_{\text{inter}} = 0) = 0.33$, we can safely say that a coincidence curve as obtained can only be observed for a single quantum dot in the 3D focal volume, even without correction for the background level. In some experiments, where single CdSe quantum dots are embedded in a PMMA matrix, the small peak at $\tau_{\text{inter}} = 0$ is entirely caused by the PMMA background luminescence.²⁵ Furthermore, we have fitted our photon-coincidence measurement to a sum of single exponentials with a least-squares algorithm, taking into account the photon-coincidence background. The apparent excited-state lifetime of the free emitting quantum dot as a fit parameter gives $\tau = 1.7$ ns, which can be reproduced for that particular quantum dot in Fig. 3(b) using the MLE procedure. Local differences in the environment, dipole orientation, and individual photoluminescence quantum yield from quantum dot to quantum dot are reflected in Fig. 3(b) by the lifetime information contrasted with an excited-state lifetime mean for all quantum dots in the scan area of $\langle \tau \rangle_{\text{mean}} = 2.8$ ns.

In conclusion, we have demonstrated two-photon excitation microscopy at the single-quantum-dot level by showing the square dependency of the PL count rate versus the excitation power. Moreover, we have quantified the confocal point spread function by means of a single colloidal nanocrystal and found good agreement to our model point spread function based on an algorithm for a fast focus field calculation that takes into account evanescent field contributions for specifically polarized input fields. The 3D capability of this microscopy imaging technique can be fully explored without size deconvolution of the probe, since the CdSe quantum dot used is much smaller than the wavelength of light in this experiment and has very good photostability during the entire measurement. From raster scanning our quantum-dot sample, we have identified the local PL intensity and corresponding excited lifetime constant per pixel. Ultimately, we have been able to demonstrate photon antibunching and triggered single-photon emission at the single-entity level via two-photon excitation. This experimental scenario enables new quantum optical experiments and physical insight for nonergodic systems at

room temperature, such as colloidal quantum dots, with 3D excitation and detection capability. Moreover, the coupling of resonant optical gold antennas²⁶ with a single nanocrystal may be finely tuned to yield triggered and directional single-photon sources at room temperature with just one 2PE laser beam.

M.W. and B.R. gratefully acknowledge support by the Karlsruhe School of Optics and Photonics. The corresponding author (H.-J.E.) acknowledges support from Deutsche Forschungsgemeinschaft (DFG) with Projects No. DFG EI 442/3-1 and No. DFG EI 442/2-2.

*hans.eisler@kit.edu

- ¹M. Göppert-Mayer, *Ann. Phys. (Weinheim, Ger.)* **401**, 273 (1931).
- ²W. Denk, J. Strickler, and W. W. Webb, *Science* **248**, 73 (1990).
- ³M. A. Albota, C. Xu, and W. W. Webb, *Appl. Opt.* **37**, 7352 (1998).
- ⁴M. Rubart, *Circ. Res.* **95**, 1154 (2004).
- ⁵D. R. Larson, W. R. Zipfel, R. M. Williams, S. W. Clark, M. P. Bruchez, F. W. Wise, and W. W. Webb, *Science* **300**, 1434 (2003).
- ⁶P. Michler, A. Imamoglu, M. D. Mason, P. J. Carson, G. F. Strouse, and S. K. Buratto, *Nature (London)* **406**, 968 (2000).
- ⁷B. Lounis, H. A. Bechtel, D. Gerion, P. Alivisatos, and W. E. Moerner, *Chem. Phys. Lett.* **329**, 399 (2000).
- ⁸G. Messin, J. P. Hermier, E. Giacobino, P. Desbiolles, and M. Dahan, *Opt. Lett.* **26**, 1891 (2001).
- ⁹X. Brokmann, E. Giacobino, M. Dahan, and J. P. Hermier, *Appl. Phys. Lett.* **85**, 712 (2004).
- ¹⁰X. Wang, X. Ren, K. Kahen, M. A. Hahn, M. Rajeswaran, S. Maccagnano-Zacher, J. Silox, G. E. Cragg, A. L. Efros, and T. D. Krauss, *Nature (London)* **459**, 686 (2009).
- ¹¹I. M. Every, *J. Phys. A: Math. Gen.* **8**, L69 (1975).
- ¹²A. Bandilla and H.-H. Ritze, *Ann. Phys. (Weinheim, Ger.)* **488**, 207 (1976).
- ¹³H. Paul, U. Mohr, and W. Brunner, *Opt. Commun.* **17**, 145 (1976).
- ¹⁴V. C. Sundar, H.-J. Eisler, and M. G. Bawendi, *Adv. Mater. (Weinheim, Ger.)* **14**, 739 (2002).
- ¹⁵G. P. Hildred and A. G. Hall, *J. Phys. A: Math. Gen.* **11**, L209 (1978).
- ¹⁶J. L. O'Brien, *Science* **318**, 1567 (2007).
- ¹⁷N. Gisin, G. Ribordy, W. Tittel, and H. Zbinden, *Rev. Mod. Phys.* **74**, 145 (2002).
- ¹⁸M. D. Wissert, K. S. Ilin, M. Siegel, U. Lemmer, and H.-J. Eisler, *Nano Lett.* **10**, 4161 (2010).
- ¹⁹R. Hanbury Brown and R. Q. Twiss, *Nature (London)* **178**, 1046 (1956).
- ²⁰M. Nirmal, B. O. Dabbousi, M. G. Bawendi, J. J. Macklin, J. Trautman, T. D. Harris, and L. E. Brus, *Nature (London)* **383**, 802 (1996).
- ²¹M. Leutenegger, R. Rao, R. A. Leitgeb, and T. Lasser, *Opt. Express* **14**, 11277 (2006).
- ²²M. D. Wissert, K. S. Ilin, M. Siegel, U. Lemmer, and H.-J. Eisler, *Nanoscale* **2**, 1018 (2010).
- ²³B. Fisher, J. M. Caruge, D. Zehnder, and M. Bawendi, *Phys. Rev. Lett.* **94**, 087403 (2005).
- ²⁴S. Felekyan, R. Kühnemuth, V. Kudryavtsev, C. Sandhagen, W. Becker, and C. A. M. Seidel, *Rev. Sci. Instrum.* **76**, 083104 (2005).
- ²⁵C. Vion, P. Spinicelli, L. Coolen, C. Schwob, J. M. Frigerio, J.-P. Hermier, and A. Maître, *Opt. Express* **18**, 7440 (2010).
- ²⁶P. Mühlischlegel, H.-J. Eisler, O. J. F. Martin, D. W. Pohl, and B. Hecht, *Science* **308**, 1607 (2005).